

Performance Analysis of Massive MIMO for Cell-Boundary Users

Yeon-Geun Lim, *Student Member, IEEE*, Chan-Byoung Chae, *Senior Member, IEEE*, and Giuseppe Caire, *Fellow, IEEE*

Abstract—In this paper, we consider massive multiple-input multiple-output (MIMO) systems for both downlink and uplink scenarios, where three radio units (RUs) connected via one digital unit (DU) support multiple user equipments (UEs) at the cell-boundary through the same radio resource, i.e., the same time-frequency slot. Zero-forcing (ZF) and maximum ratio transmission (MRT) are considered as downlink transmitter options, while ZF and maximum ratio combining (MRC) are considered as uplink receiver options. We derive simple closed-form formulas for the sum rate of each such technique. Based on our analytical results, for the downlink, we observe that vector normalization is better for ZF while matrix normalization is better for MRT, in the simple but practically relevant case where uniform power is allocated to all downlink data streams. For a given antenna and users configuration, we also derive analytically the SNR level below which MRC should be used instead of ZF. Numerical simulations confirm our analytical results.

Index Terms—Massive MIMO, cell-boundary users, ergodic achievable rate, matched filter, zero-forcing, normalization, precoding, and combining filter.

I. INTRODUCTION

Multiple-input multiple-output (MIMO) wireless communication techniques have evolved from single-user MIMO (SU-MIMO) to multi-user MIMO (MU-MIMO) systems [1]. To approach the capacity of the MIMO broadcast channel, [2], [3] proposed simple zero-forcing (ZF) based-linear algorithms, where the transmitter and the receivers are equipped with multiple antennas. The optimality of the linear matched type combining filter was intensively investigated in [4] with the assumption of an infinite number of antennas at the receiver. In particular, [4] proves that a simple linear beamforming (coordinated beamforming in the paper) asymptotically approaches the sum capacity achieved by dirty paper coding (DPC).

Recently, massive MIMO (a.k.a. large-scale MIMO) has been proposed to further maximize network capacity and to conserve energy [5]–[7]. In [6], massive MIMO systems using simple linear algorithms such as the maximum ratio combining (MRC) for the uplink and the maximum ratio transmission (MRT) for the downlink are proposed. To further maximize the network capacity, several network MIMO algorithms with multiple receive antennas have been proposed [8], [9]. These systems assume, however, that the network supports a maximum of three users through a relatively small number of

transmit antennas.¹

Massive MIMO systems in multi-cell environments were also studied in [5], [7], [10], [11]. Multi-cell massive MIMO has some critical issues, such as pilot contamination, that becomes the main capacity-limiting factor in time division duplex (TDD) systems, especially when MRT is used. Joint spatial division and multiplexing is proposed in [12] to employ frequency division duplex (FDD) systems. The authors in [13] proposed a pilot alignment algorithm for a cognitive massive MIMO system. The authors in [7] investigated downlink performance with MRT and ZF precoder for a massive MIMO system.² In [5], the authors studied uplink performance with MRC, ZF, minimum mean square error (MMSE) filter for massive MIMO. It was shown that transmit energy can be conserved by a power-scaling law $1/M$ with perfect channel state information (CSI) and $1/\sqrt{M}$ with imperfect CSI at the base station (BS), where M represents the number of BS antennas. In [11], the authors showed theoretically and numerically the impact of pilot contamination and proposed a multi-cell MMSE-based precoding algorithm to reduce both intra- and inter-cell interference. In [11], MRT precoding was used; the inter-user interference is eventually eliminated once the transmitter has a large enough number of antennas.

The assumption of an infinite number of antennas at the BS for a finite number of users somehow trivializes many problems (e.g., in this limit MRC/MRT have the same performance of ZF). A more meaningful system scaling is considered in [10], [15], [16], where the number of antennas per BS and the number of users both go to infinity with fixed ratio. In this case, the infinite number of BS antenna per user results can be recovered by letting this ratio become large. This more refined analysis, however, illuminates the all the system performance regimes. For example, in [16] the “massive MIMO” regime is defined as the regime where pilot contamination dominates with respect to multiuser interference, and it is noticed that this regime occurs only when the number of BS antennas per user is impractically large. These conclusions are also reached, independently and in parallel, in [10]. In particular, [10] considers a multi-cell architecture formed by small clusters of cooperating BSs. They proposed a system where the users are partitioned into homogeneous classes and the downlink MIMO precoding scheme is optimized for each class. Then, a scheduler optimally allocates the time-frequency transmission

Y.-G. Lim and C.-B. Chae are with the School of Integrated Technology, Yonsei University, Korea. Email: {yglm, cbchae}@yonsei.ac.kr. G. Caire is with Department of Electrical Engineering, University of Southern California, USA. Email: caire@usc.edu.

¹Note that more than three users can be supported if there is a common message, i.e., for a clustered broadcast channel.

²In [14], the authors investigated the performance of MRT and ZF in large-scale antenna systems, but did not pay attention to normalization techniques.

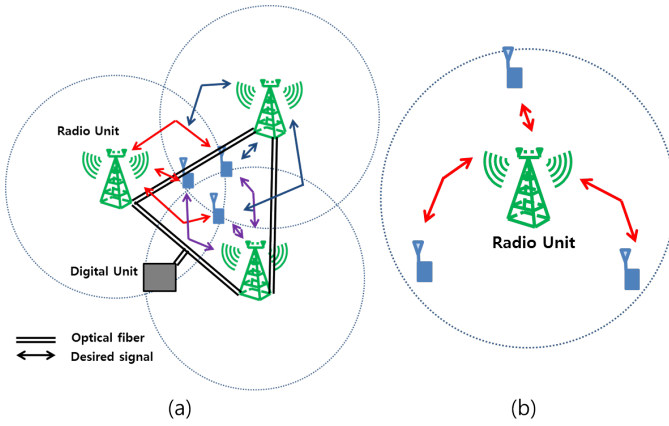


Fig. 1. (a) System model of multi-RU massive MIMO scenario with cell-boundary users. (b) System model of single-RU massive MIMO scenario with cell-boundary users.

resource across the different user classes, yielding an inherent multi-mode multi-cell massive MIMO system. One of the main outcomes of [10] is that it is convenient to serve users at the cell center in a single-cell mode, while users at the cell edge should be served by small cooperative clusters formed by the closest three neighboring cell/sectors.

Motivated by the results in [10], in this paper we focus on the edge-cell user performance, which is the system bottleneck both for the uplink and for the downlink. The massive MIMO system under consideration consists of multiple radio units (RUs) connected with one another by optical fibers, and further connected to a centralized digital unit (DU), as illustrated in Figs. 1(a) and 2.³ Through the optical fibers, each RU can share data messages and channel state information. Since the cell edge users have symmetric and spatially isotropic channel statistics with respect to all three neighboring BSs forming a cluster, the system is equivalent to a single-cell massive MIMO system as shown in Fig. 1(b). As in the above referenced previous works, we consider the performance of linear precoding/filtering schemes such as ZF and MRT for the downlink and ZF and MRC for the uplink. In particular, we consider two possible normalization of the precoding filters for the downlink, referred to as vector or matrix normalization. The main contributions of this paper are as follows:

- **Ergodic achievable sum rate of ZF and MRT/MRC:**

We derive simple approximations for the ergodic achievable sum rate of ZF and MRT/MRC. These approximations are accurate and far simpler to evaluate than the *exact asymptotic expressions* given in [10], [15], [16], obtained through asymptotic random matrix theory [17] and usually given in terms of the solution of multiple coupled fixed-point equations. Thanks to their simplicity, the proposed approximations are suitable to analyze the low and high SNR regimes. Numerical results demonstrate the tightness of our analysis.

- **Downlink precoding normalization methods:** We compare matrix and vector normalization for down-

link precoding, in the simple and practical case of uniform power allocation over all downlink streams. It is well-known that with optimal (waterfilling) power allocation and ZF precoding these normalizations yield identical results [18]. However, with practical suboptimal power allocation and in the finite antenna regime these normalizations are generally not equivalent. Most prior work on multiuser MIMO paid little attention to this issue. Using the *arithmetic-geometric inequality*, we find that vector normalization performs better for ZF precoding, while matrix normalization performs better for MRT precoding.

- **Transceiver mode selection algorithms:** We propose two transceiver mode selection algorithms as a function of SNR and the number of active users per BS antenna. In [19], it is concluded that ZF is better for cell center users, i.e., high signal-to-noise-ratio (SNR), and MRT is better for cell-boundary users, i.e., low SNR, in a downlink system. However, [19] did not consider transceiver mode selection as function of SNR (i.e., of the transmit power, for a given pathloss law and cell geometry) for the same class of edge users. In this paper, we explain how much transmit power and/or number of active users are needed for ZF to provide a better sum rate than MRT (for downlink) or MRC (for uplink). In particular, we find the optimal MIMO mode selection scheme in terms of closed-form thresholds of the transmit power, where the thresholds depend on the number of edge users.

This paper is organized as follows. In Section II, we introduce the considered system model and problem statement with respect to precoding normalization methods and beamforming techniques. In Section III, we introduce some mathematical preliminaries useful for analysis. In Section IV, we analyze i) the sum rate lower and upper bounds, ii) the ergodic performance of ZF- and MRT-precoding, and iii) which precoding normalization method is better for each precoder. In Section V, we provide an approximation of the achievable ergodic sum rate. In Section VI, we propose transceiver mode selection algorithms with i) a power threshold, and ii) number of users cross point of ZF- and MRT- precoding techniques. Numerical results are shown in Section VII. Section VIII presents our conclusions and future work.

II. SYSTEM MODEL AND PROBLEM STATEMENT

In this section, we introduce the basic notation used in this paper and the massive MIMO system model.⁴

A. System Model: Network Massive MIMO

⁴Throughout this paper, we use upper and lower case boldfaces to describe matrix \mathbf{A} and vector \mathbf{a} , respectively. We denote the inverse, transpose and the Hermitian of matrix \mathbf{A} by \mathbf{A}^{-1} , \mathbf{A}^T and \mathbf{A}^* , respectively. $\|\mathbf{A}\|_F$ indicates the Frobenius norm of matrix \mathbf{A} . The notations of expectation, variance, and covariance are represented by \mathbb{E} , Var , and Cov respectively.

³To avoid confusion, we use RU instead of base station hereafter.

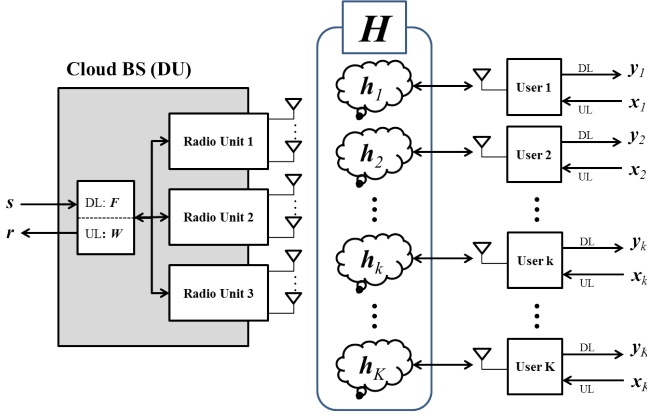


Fig. 2. Block diagram of multi-RU massive MIMO system. One DU consists of three RUs connected by optical fibers. This model is regarded as a single-RU massive MIMO system.

Consider a massive MIMO system as shown in Figs. 1 and 2. One DU (cloud BS) controls three RUs and K users. Each RU is connected with one another by optical fibers. Fig. 1(a) shows that the cloud BS provides a massive MIMO environment to cell-edge users under the assumption that RU has a relatively small number of antennas (more practical in the recent antenna configuration; we will use this system model in Section VII). Fig. 1(b) illustrates the equivalent model of Fig. 1(a) considered as single-cell massive MIMO systems. We assume that the cloud BS has M antennas and each user equipment (UE) is equipped with one antenna. In this paper, we do not consider pilot contamination and assume perfect CSI at the RU. We also assume that the channel is flat fading and the elements of a channel matrix are modeled as independent complex Gaussian random variables with zero mean and unit variance. The channel between the cloud BS (one DU and three RUs) and the k -th user is denoted by an $1 \times M$ row vector \mathbf{h}_k^T ($k = 1, 2, \dots, K$). A $K \times M$ channel matrix \mathbf{H} between the cloud BS and all UEs consists of channel vectors \mathbf{h}_k^T . Let \mathbf{g}_k denote the column vector of transmit precoding and s_k represent the transmit symbol for the k -th UE at downlink. Similarly, let \mathbf{w}_k denote the column vector of receive combining filter for the k -th UE at uplink. Also, let n_k be the additive white Gaussian noise vector. Then, the received signal at the k -th UE is expressed by

$$y_k = \underbrace{\sqrt{P_t} \mathbf{h}_k^T \mathbf{g}_k s_k}_{\text{desired signal}} + \underbrace{\sum_{\ell=1, \ell \neq k}^K \sqrt{P_t} \mathbf{h}_k^T \mathbf{g}_\ell s_\ell}_{\text{interference}} + n_k \quad (1)$$

where, P_t denotes the total network transmit power across three RUs. Also, the received signal for the k -th UE at the cloud BS is expressed by

$$r_k = \underbrace{\sqrt{P_u} \mathbf{w}_k^T \mathbf{h}_k x_k}_{\text{desired signal}} + \underbrace{\sum_{\ell=1, \ell \neq k}^K \sqrt{P_u} \mathbf{w}_k^T \mathbf{h}_\ell x_\ell}_{\text{interference}} + n_k \quad (2)$$

where, P_u and x_k denote the transmit power per each user and the transmit symbol of the k -th user at uplink, respectively.

B. Problem Statement: Downlink

Eq. (1) contains the desired signal, interference, and noise terms. To eliminate the interference term, we use the following precoding:

$$\text{ZF} : \mathbf{F} = \mathbf{H}^* (\mathbf{H} \mathbf{H}^*)^{-1} = [\mathbf{f}_1 \ \mathbf{f}_2 \ \dots \ \mathbf{f}_k \ \dots \ \mathbf{f}_K],$$

$$\text{MRT} : \mathbf{F} = \mathbf{H}^* = [\mathbf{f}_1 \ \mathbf{f}_2 \ \dots \ \mathbf{f}_k \ \dots \ \mathbf{f}_K]$$

where \mathbf{F} is a precoding matrix consisting of each column vector \mathbf{f}_k .

To satisfy the power constraint, we need to normalize the precoding matrix. As mentioned above, we consider two methods, i.e., vector/matrix normalizations. The normalized transmit beamforming vectors (columns of a precoding matrix) with vector/matrix normalizations are given as $\mathbf{g}_k = \mathbf{f}_k / (\sqrt{K} \|\mathbf{f}_k\|)$ and $\mathbf{g}_k = \mathbf{f}_k / \|\mathbf{F}\|_F$, respectively. Note that vector normalization imposes equal power per downlink stream, while matrix normalization yields streams with different power. In this paper, to simplify, we do not consider a power optimization that could yield a complexity problem in very large array antenna systems.

1) *ZF/MRT with vector normalization*: The received signal at the k -th UE can be expressed as follows:

$$y_k = \sqrt{P_t} \mathbf{h}_k^T \frac{\mathbf{f}_k}{\sqrt{K} \|\mathbf{f}_k\|} s_k + \sum_{\ell=1, \ell \neq k}^K \sqrt{P_t} \mathbf{h}_k^T \frac{\mathbf{f}_\ell}{\sqrt{K} \|\mathbf{f}_\ell\|} s_\ell + n_k. \quad (3)$$

2) *ZF/MRT with matrix normalization*: Similarly, we can rewrite the received signal with matrix normalization as such:

$$y_k = \sqrt{P_t} \mathbf{h}_k^T \frac{\mathbf{f}_k}{\|\mathbf{F}\|_F} s_k + \sum_{\ell=1, \ell \neq k}^K \sqrt{P_t} \mathbf{h}_k^T \frac{\mathbf{f}_\ell}{\|\mathbf{F}\|_F} s_\ell + n_k. \quad (4)$$

C. Problem Statement: Uplink

Similar to the downlink system, to eliminate the interference term, and to maximize the SNR in (2), we use the following combining filter at the RUs:

$$\text{ZF} : \mathbf{W} = (\mathbf{H}^* \mathbf{H})^{-1} \mathbf{H}^* = [\mathbf{w}_1 \ \mathbf{w}_2 \ \dots \ \mathbf{w}_k \ \dots \ \mathbf{w}_K],$$

$$\text{MRC} : \mathbf{W} = \mathbf{H}^* = [\mathbf{w}_1 \ \mathbf{w}_2 \ \dots \ \mathbf{w}_k \ \dots \ \mathbf{w}_K]$$

where \mathbf{W} is a combining filter matrix consisting of each column vector \mathbf{w}_k . Here, we do not consider normalization since it does not change SNR values in the uplink scenario.

D. Achievable Rate Bound

In this paper, to maximize the achievable sum rate of downlink/uplink systems, we evaluate the closed forms of each system's performance. The achievable rates are bounded as follows:

$$\begin{aligned} \log_2 \left\{ 1 + \frac{1}{\mathbb{E} \left(\frac{I+N}{S} \right)} \right\} &\leq \mathbb{E} \left\{ \log_2 \left(1 + \frac{S}{I+N} \right) \right\} \\ &\leq \log_2 \left\{ 1 + \mathbb{E} \left(\frac{S}{I+N} \right) \right\} \end{aligned}$$

by using *Jensen's Inequality* of convex and concave functions where S , I , and N represent signal power, interference power,

and noise power, respectively. Note that we use these bounds only for ZF cases and show that our results, based on the bounds, are more accurate than prior work [5], [7], [16].

III. MATHEMATICAL PRELIMINARIES

In this section, we introduce some mathematical preliminaries to evaluate an asymptotic analysis for network massive MIMO, which will be used in Sections IV and V.

A. Expectation and Variance of Random Vectors

Lemma 1: Let \mathbf{h}_k and \mathbf{h}_ℓ ($k \neq \ell$) be $M \times 1$ vectors whose elements are independent identically distributed (i.i.d.) complex Gaussian random variables with zero mean and unit variance.

- 1) $\mathbb{E}[|\mathbf{h}_k|^2] = M$,
 $\text{Var}[|\mathbf{h}_k|^2] = M$.
- 2) $\mathbb{E}[\mathbf{h}_k^* \mathbf{h}_\ell] = 0$,
 $\text{Var}[\mathbf{h}_k^* \mathbf{h}_\ell] = M$.
- 3) $\mathbb{E}[|\mathbf{h}_k|^4] = M^2 + M$,
 $\text{Var}[|\mathbf{h}_k|^4] = 4M^3 + 10M^2 + 6M$.
- 4) $\mathbb{E}[\mathbf{h}_k^* \mathbf{h}_\ell^2] = M$,
 $\text{Var}[\mathbf{h}_k^* \mathbf{h}_\ell^2] = M^2 + 2M$.

Proof: See Appendix A

B. Effective Channel

Lemma 2: In massive MIMO systems, transmit energy can be conserved by power-scaling law $1/M$ with perfect CSI.

- 1) $\lim_{M \rightarrow \infty} \mathbb{E}[\frac{1}{M} |\mathbf{h}_k|^2] = 1$,
 $\lim_{M \rightarrow \infty} \text{Var}[\frac{1}{M} |\mathbf{h}_k|^2] = 0$.
- 2) $\lim_{M \rightarrow \infty} \mathbb{E}[\frac{1}{M} \mathbf{h}_k^* \mathbf{h}_\ell] = 0$,
 $\lim_{M \rightarrow \infty} \text{Var}[\frac{1}{M} \mathbf{h}_k^* \mathbf{h}_\ell] = 0$.

Generally, a transceiver uses MRT or MRC in massive MIMO, which means that the effective channel of the desired signal becomes one and the interference signal becomes zero as the number of antennas (M) goes to infinity, as illustrated:

$$\frac{1}{M} \mathbf{H} \mathbf{H}^* \xrightarrow{a.s.} \mathbf{I}_K, \text{ as } M \rightarrow \infty$$

where the diagonal term of the effective channel matrix becomes deterministic because its variance goes to zero by *Lemma 2* as well as the off-diagonal term becomes deterministic.

C. Signal and Interference Power

Lemma 3: In a similar way, the expectation and the variance of the signal and the interference power are given by

- 1) $\lim_{M \rightarrow \infty} \mathbb{E}[\frac{1}{M^2} |\mathbf{h}_k|^4] = 1$,
 $\lim_{M \rightarrow \infty} \text{Var}[\frac{1}{M^2} |\mathbf{h}_k|^4] = 0$.
- 2) $\lim_{M \rightarrow \infty} \mathbb{E}[\frac{1}{M^2} \mathbf{h}_k^* \mathbf{h}_\ell^2] = 0$,
 $\lim_{M \rightarrow \infty} \text{Var}[\frac{1}{M^2} \mathbf{h}_k^* \mathbf{h}_\ell^2] = 0$.

Note that the terms $\frac{1}{M} |\mathbf{h}_k|^4$ and $\frac{1}{M} \mathbf{h}_k^* \mathbf{h}_\ell^2$ do not converge to M and zero, respectively, as M goes to infinity since their variance does not go to zero, which means that they still have randomness.

D. Chebyshev's Inequality

Lemma 4: Let X be a random variable with variance σ_X^2 , c be a scalar, and $Y = \frac{1}{c}X$ be a random variable with variance $\sigma_Y^2 = \frac{1}{c^2} \sigma_X^2$, respectively. If c is relatively larger than σ_X , then σ_Y is almost zero, i. e.,

$$\text{if } \sigma_Y = 0,$$

$$\text{then } P[Y = \mathbb{E}\{Y\}] = 1$$

by *Chebyshev's Inequality*. We use this *Lemma* to approximate a signal-to-interference-plus-noise-ratio (SINR) term in ergodic sum rate expressions.

As an example, to analyze the rate in the high SNR regime, from *Lemma 1* and *4*, if $\text{Var}[\frac{1}{P_t} |\mathbf{h}_k|^2] = \frac{1}{P_t^2} M \xrightarrow{a.s.} 0$ where $P_t \geq M$ as M goes to infinity, then $\frac{1}{P_t} |\mathbf{h}_k|^2 \xrightarrow{a.s.} \frac{1}{P_t} \mathbb{E}[|\mathbf{h}_k|^2] = \frac{1}{P_t} M$. Note that $\text{Var}[\frac{1}{P_t} |\mathbf{h}_k|^4]$ does not converge to zero as M goes to infinity.

E. Ergodic Achievable Sum Rate of Massive MIMO Systems

Lemma 5: Let X_v and v_i be a norm of random vector \mathbf{v} ($M \times 1$) and the i -th entry of \mathbf{v} , respectively, i. e., $X_v = v_1^2 + v_2^2 + \dots + v_M^2$. Since $\mathbb{E}\left\{\frac{1}{X_v}\right\} = \mathbb{E}\left\{\frac{1}{v_1^2 + v_2^2 + \dots + v_M^2}\right\}$ and $\frac{1}{\mathbb{E}\{X_v\}} = \frac{1}{\mathbb{E}\{v_1^2 + v_2^2 + \dots + v_M^2\}}$, $\mathbb{E}\left\{\frac{1}{X_v}\right\}$ converges to $\frac{1}{\mathbb{E}\{X_v\}}$ as M goes to infinity. In this *Lemma*, we assume that a desired signal term or an interference plus noise term has the same property of X_v , and also satisfies a condition of *Lemma 4*. If $S \xrightarrow{a.s.} \mathbb{E}\{S\}$ from *Lemma 4*, then $\mathbb{E}\left\{\frac{S}{I+N}\right\} \xrightarrow{a.s.} \mathbb{E}\{S\} \mathbb{E}\left\{\frac{1}{I+N}\right\} \xrightarrow{a.s.} \frac{\mathbb{E}\{S\}}{\mathbb{E}\{I+N\}}$ as M goes to infinity. Similarly, for $I+N \xrightarrow{a.s.} \mathbb{E}\{I+N\}$ cases, we also obtain $\mathbb{E}\left\{\frac{S}{I+N}\right\} \xrightarrow{a.s.} \frac{\mathbb{E}\{S\}}{\mathbb{E}\{I+N\}}$. So we could obtain the following approximation of SINR:

$$\mathbb{E}\left\{\frac{S}{I+N}\right\} \approx \frac{\mathbb{E}(S)}{\mathbb{E}(I+N)}. \quad (5)$$

From (5), the lower bound of the ergodic sum rate is the same as the upper bound of the ergodic sum rate. Thus we could also get the following approximation of the ergodic sum rate when M goes to infinity at the low or high SNR regime:

$$\mathbb{E}\left(\log_2\left(1 + \frac{S}{I+N}\right)\right) \approx \log_2\left(1 + \frac{\mathbb{E}(S)}{\mathbb{E}(I+N)}\right).$$

F. Arithmetic-Geometric Inequality

Lemma 6: Let a_1, a_2, \dots, a_K be variables of a concave function, and b_k be scaled variables, i.e., $a_k = Kb_k$. We can obtain the following inequality through *Arithmetic-geometric Inequality* defined in [20]:

$$\sum_{k=1}^K \log_2\left(1 + \frac{1}{Kb_k}\right) \geq K \log_2\left(1 + \frac{1}{\sum_{k=1}^K b_k}\right).$$

Proof:

$$\begin{aligned} \frac{1}{K} \sum_{k=1}^K \log_2 \left(1 + \frac{1}{K b_k} \right) &\geq \log_2 \left(1 + \frac{1}{\frac{1}{K} \sum_{k=1}^K K b_k} \right) \\ \Leftrightarrow \sum_{k=1}^K \log_2 \left(1 + \frac{1}{K b_k} \right) &\geq K \log_2 \left(1 + \frac{1}{\sum_{k=1}^K b_k} \right). \end{aligned} \quad (6)$$

by applying *Jensen's Inequality*. ■

IV. ASYMPTOTIC DOWNLINK SUM RATE

In this section, we derive the achievable rate bounds, and show which normalization method is suitable for ZF- and MRT-type precoding at the downlink. Based on our analytical results, we will also show which precoding technique is desired for cell-boundary users.

A. Ergodic Performance of ZF precoding

The lower bound of the ergodic sum rate for the ZF precoding case is well known, as follows [5]:

$$\mathcal{R}_{\text{ZFvec}, \text{DL}}^L = \mathcal{R}_{\text{ZFmat}, \text{DL}}^L = K \log_2 \left\{ 1 + \frac{P_t(M-K+1)}{K} \right\}$$

using the property of Wishart matrices [17].

1) *Vector normalization-upper bound:* From (3), we can derive the SINR of the upper bound of vector normalization in the ZF case, as given by

$$\begin{aligned} \mathbb{E} \left\{ \frac{S}{I+N} \right\} &= \mathbb{E} \left\{ \frac{P_t \left| \mathbf{h}_k^T \frac{\mathbf{f}_k}{\sqrt{K} \|\mathbf{f}_k\|} \right|^2}{P_t \sum_{\ell=1, \ell \neq k}^K \left| \mathbf{h}_k^T \frac{\mathbf{f}_\ell}{\sqrt{K} \|\mathbf{f}_\ell\|} \right|^2 + 1} \right\} \\ &= \mathbb{E} \left\{ \frac{P_t}{K \|\mathbf{f}_k\|^2} \right\} \\ &\stackrel{(c)}{=} \frac{P_t(M-K+1)}{K} \end{aligned} \quad (7)$$

where (c) results from the diversity order of ZF, as shown in [21]. From (7), the upper bound of vector normalization in the ZF case can be represented as

$$\mathcal{R}_{\text{ZFvec}, \text{DL}}^U = K \log_2 \left\{ 1 + \frac{P_t(M-K+1)}{K} \right\}.$$

2) *Matrix normalization-upper bound:* From (4), the SINR of the upper bound of matrix normalization in the ZF case can be expressed as

$$\begin{aligned} \mathbb{E} \left\{ \frac{S}{I+N} \right\} &= \mathbb{E} \left\{ \frac{P_t \left| \mathbf{h}_k^T \frac{\mathbf{f}_k}{\|\mathbf{F}\|_F} \right|^2}{P_t \sum_{\ell=1, \ell \neq k}^K \left| \mathbf{h}_k^T \frac{\mathbf{f}_\ell}{\|\mathbf{F}\|_F} \right|^2 + 1} \right\} \\ &= \mathbb{E} \left\{ P_t \left| \frac{1}{\|\mathbf{F}\|_F} \right|^2 \right\}. \end{aligned} \quad (8)$$

From (8), the first upper bound (with an expectation form) of matrix normalization in the ZF case can be represented as

$$\mathcal{R}_{\text{ZFmat}, \text{DL}}^{U1} = K \log_2 \left\{ 1 + \mathbb{E} \left(P_t \left| \frac{1}{\|\mathbf{F}\|_F} \right|^2 \right) \right\}. \quad (9)$$

By using *Lemma 6*, (9) can further be expressed as

$$\begin{aligned} &K \log_2 \left\{ 1 + \mathbb{E} \left(P_t \left| \frac{1}{\|\mathbf{F}\|_F} \right|^2 \right) \right\} \\ &= K \log_2 \left\{ 1 + \mathbb{E} \left(P_t \frac{1}{\text{tr}((\mathbf{H}\mathbf{H}^*)^{-1})} \right) \right\} \\ &= K \log_2 \left\{ 1 + \mathbb{E} \left(P_t \frac{1}{\sum_{k=1}^K \|\mathbf{f}_k\|^2} \right) \right\} \\ &\leq K \log_2 \left\{ 1 + \mathbb{E} \left(P_t \frac{1}{K \|\mathbf{f}_k\|^2} \right) \right\}. \end{aligned}$$

So the second upper bound (without an expectation form) of matrix normalization in the ZF case can be given by

$$\mathcal{R}_{\text{ZFmat}, \text{DL}}^{U2} = K \log_2 \left\{ 1 + \frac{P_t(M-K+1)}{K} \right\}. \quad (10)$$

3) *Ergodic achievable sum rate of ZF at low SNR regime:* We assume that the transmit power (P_t) is small for cell-boundary users (low SNR regime). Using the property of ZF precoding, the ergodic achievable sum rate of ZF is represented as

$$\begin{aligned} \mathbb{E} \left\{ \log_2 \left(1 + \frac{S}{I+N} \right) \right\} &= \mathbb{E} \left\{ \log_2 (1 + P_t \mathbf{h}_k^T \mathbf{g}_k) \right\} \\ &\stackrel{(a)}{\approx} \log_2 \{ 1 + P_t \mathbb{E}(\mathbf{h}_k^T \mathbf{g}_k) \} \end{aligned} \quad (11)$$

where (a) results from *Lemma 4*. Eq. (11) indicates that the achievable sum rate of ZF precoding can approach its upper bounds at low SNR by *Lemma 4*. Thus the ergodic achievable sum rate of ZF with vector normalization at low SNR is given by

$$\mathcal{R}_{\text{ZFvec}, \text{DL}} = K \log_2 \left\{ 1 + \frac{P_t(M-K+1)}{K} \right\}.$$

Also, the ergodic achievable sum rate of ZF with matrix normalization at low SNR is given by

$$\mathcal{R}_{\text{ZFmat}, \text{DL}} = K \log_2 \left\{ 1 + \mathbb{E} \left(P_t \left| \frac{1}{\|\mathbf{F}\|_F} \right|^2 \right) \right\}.$$

4) *ZF performance for the case $M = K$:* We derive the ergodic sum rate of ZF with vector normalization at low SNR (or lower bound of ZF with vector normalization) when $M = K$

$$\begin{aligned} \lim_{M \rightarrow \infty} \mathcal{R}_{\text{ZFvec}, \text{DL}}(M=K) &= \lim_{K \rightarrow \infty} K \log_2 \left\{ 1 + \frac{P_t}{K} \right\} \\ &= \lim_{K \rightarrow \infty} P_t \log_2 e \ln \left\{ 1 + \frac{P_t}{K} \right\}^{K/P_t} \\ &= P_t \log_2 e. \end{aligned} \quad (12)$$

This is equal to the result in [22]. From this result, we are able to gather insights into user scheduling, which will be discussed in Section VI.

5) *Performance comparison of ZF*: To find which normalization technique is better in ZF, we let $b_k = \frac{[(\mathbf{H}\mathbf{H}^*)^{-1}]_{kk}}{P_t}$ in Lemma 6 directly.

$$\begin{aligned} & \sum_{k=1}^K \log_2 \left(1 + \frac{P_t}{K[(\mathbf{H}\mathbf{H}^*)^{-1}]_{kk}} \right) \\ & \geq K \log_2 \left(1 + \frac{P_t}{\sum_{k=1}^K [(\mathbf{H}\mathbf{H}^*)^{-1}]_{kk}} \right) \\ & \Leftrightarrow \mathcal{R}_{\text{ZF}, \text{vec}, \text{DL}} \geq \mathcal{R}_{\text{ZF}, \text{mat}, \text{DL}}. \end{aligned} \quad (13)$$

From (13), we can conclude that, in the ZF case, vector normalization is always better than matrix normalization.

B. Ergodic Performance of MRT precoding

1) *Vector normalization-low SNR regime*: From (3), we can derive the ergodic achievable sum rate of vector normalization in low SNR as follows:

$$\mathcal{R}_{\text{MRT}, \text{vec}, \text{DL-L}} \approx K \log_2 \left\{ 1 + \frac{P_t M}{P_t(K-1) + K} \right\} \quad (14)$$

Proof: See Appendix B1. ■

2) *Vector normalization-high SNR regime*: Similarly, we can get the achievable sum rate of vector normalization in high SNR as follows:

$$\mathcal{R}_{\text{MRT}, \text{vec}, \text{DL-H}} \approx K \log_2 \left\{ 1 + \frac{P_t(M+1)}{P_t(K-1) + K} \right\} \quad (15)$$

Proof: See Appendix B2. ■

3) *Matrix normalization-low/high SNR regime*: From (4), we can evaluate the ergodic achievable sum rate of matrix normalization in low/high SNR by using the following formation:

$$\mathcal{R}_{\text{MRT}, \text{mat}, \text{DL-L/H}} \approx K \log_2 \left\{ 1 + \frac{P_t(M+1)}{P_t(K-1) + K} \right\} \quad (16)$$

Proof: See Appendix B3 and B4. ■

4) *Performance comparison of MRT*: From (14)-(16), a comparison of the ergodic achievable sum rate is given by

$$\mathcal{R}_{\text{MRT}, \text{mat}, \text{DL-L}} > \mathcal{R}_{\text{MRT}, \text{vec}, \text{DL-L}} \quad (17)$$

at low SNR, and

$$\mathcal{R}_{\text{MRT}, \text{mat}, \text{DL-H}} \approx \mathcal{R}_{\text{MRT}, \text{vec}, \text{DL-H}} \quad (18)$$

at high SNR. From (17) and (18), we confirm that, for MRT precoding, matrix normalization is always better than vector normalization at low SNR. We conclude, however, that there is no performance gap between vector normalization and matrix normalization at high SNR.

V. ASYMPTOTIC UPLINK SUM RATE

We have focused on a downlink scenario with a sum power constraint. In this section, we investigate an uplink case, where each user has an its own power constraint. From (2), the ergodic achievable sum rate for the uplink, \mathcal{R}_{UL} , is

$$\mathcal{R}_{\text{UL}} = \mathbb{E} \left[\sum_{k=1}^K \log_2 \left\{ 1 + \frac{P_u |\mathbf{w}_k^T \mathbf{h}_k|^2}{P_u \sum_{\ell=1, \ell \neq k}^K |\mathbf{w}_k^T \mathbf{h}_\ell|^2 + |\mathbf{w}_k|^2} \right\} \right]. \quad (19)$$

From (19), we can derive the ergodic achievable uplink sum rate of MRC, $\mathcal{R}_{\text{MRC}, \text{UL}}$, as follows:

$$\begin{aligned} & \mathcal{R}_{\text{MRC}, \text{UL}} \\ & = \mathbb{E} \left[\sum_{k=1}^K \log_2 \left\{ 1 + \frac{P_u |\mathbf{h}_k|^4}{P_u \sum_{\ell=1, \ell \neq k}^K |\mathbf{h}_k^* \mathbf{h}_\ell|^2 + |\mathbf{h}_k|^2} \right\} \right]. \end{aligned} \quad (20)$$

We approximate the ergodic achievable sum rate of MRC as follows:

i) High SNR regime ($P_u \geq M$):

$$\mathcal{R}_{\text{MRC}, \text{UL-H}} \approx K \log_2 \left\{ 1 + \frac{P_u(M+1)}{P_u(K-1) + 1} \right\}. \quad (21)$$

ii) Low SNR regime ($P_u \leq \frac{1}{M}$):

$$\mathcal{R}_{\text{MRC}, \text{UL-L}} \approx K \log_2 \left\{ 1 + \frac{P_u M}{P_u(K-1) + 1} \right\}. \quad (22)$$

Proof: See Appendix C. ■

When the RUs have finite but large M antennas, this approximation is quite accurate. Similar to ZF precoding, the ergodic sum rate for ZF for uplink at low SNR, $\mathcal{R}_{\text{ZF}, \text{UL-L}}$, is

$$\begin{aligned} \mathcal{R}_{\text{ZF}, \text{UL-L}} & \approx \mathcal{R}_{\text{ZF}, \text{UL}}^U = K \log_2 \left\{ 1 + \mathbb{E} \left\{ \frac{P_u}{[(\mathbf{H}^* \mathbf{H})^{-1}]_{k,k}} \right\} \right\} \\ & = K \log_2 \{ 1 + P_u(M-K+1) \}. \end{aligned}$$

VI. TRANSCEIVER MODE SELECTION ALGORITHM

In this section, we propose two transceiver mode selection algorithms from i) transmit power perspective and ii) the number of active users perspective. To provide a mathematically simple solution, we first propose Lemma 7 and Lemma 8 use a power threshold as follows:

Lemma 7: The power threshold to select a better precoder for downlink is given by

$$P_{\text{th}, \text{DL}} = \frac{K^2}{(K-1)(M-K+1)}. \quad (23)$$

If the RUs have more transmit power than the power threshold $P_{\text{th}, \text{DL}}$, the ZF precoder provides a better sum rate performance.

Proof: To derive (23) for cell-boundary users, we use the low SNR approximation for ZF and MRT. By letting $\mathcal{R}_{\text{ZF}, \text{vec}, \text{DL-L}} \geq \mathcal{R}_{\text{MRT}, \text{mat}, \text{DL-L}}$, we can get (23) as follows:

$$\begin{aligned} & \mathcal{R}_{\text{ZF}, \text{vec}, \text{DL-L}} - \mathcal{R}_{\text{MRT}, \text{mat}, \text{DL-L}} \geq 0 \\ & \Leftrightarrow \frac{P_t(M-K+1)}{K} - \frac{P_t(M+1)}{P_t(K-1) + K} \geq 0 \\ & \Leftrightarrow P_t \geq P_{\text{th}, \text{DL}} = \frac{K^2}{(K-1)(M-K+1)}. \end{aligned}$$

Lemma 8: The power threshold to select a better receive combining filter at uplink is given by

$$P_{\text{th}, \text{UL}} = \frac{1}{M-K+1}. \quad (24)$$

If each UE has larger transmit power per user than $P_{\text{th, UL}}$, the solution employing ZF at the RUs provides a better sum rate performance.

Proof: To evaluate (24), we use the low SNR approximation of MRC, i.e., (22). From $\mathcal{R}_{\text{ZF, UL}}^L \geq \mathcal{R}_{\text{MRC, UL}_L}$, we can obtain (24) for uplink as follows:

$$\begin{aligned} \mathcal{R}_{\text{ZF, UL}_L} - \mathcal{R}_{\text{MRC, UL}_L} &\geq 0 \\ \Leftrightarrow P_u(M - K + 1) - \frac{P_u M}{P_u(K - 1) + 1} &\geq 0 \\ \Leftrightarrow P_u \geq P_{\text{th, UL}} = \frac{1}{M - K + 1}. \end{aligned}$$

Lemma 7 helps the RU select one of the precoders, i.e., ZF or MRT, with respect to the transmit power of the cloud BS. Also, the power policy of the cloud BS could be adjusted by the power threshold that is a function of M and K . Therefore, the RU could find a suitable precoding mode according to the user's locations. Similarly, *Lemma 8* could be applied to the uplink case.

The proposed power threshold would be affected by a specific number of users, so a power cross point, that refers to P_{cross} , exists where MRT or MRC is always better for any number of active users. Since *Lemmas 7* and *8* are a monotonic increasing function of K , $P_{\text{th, DL}}$ and $P_{\text{th, UL}}$ have minimum values at $K = 2$. These points become $P_{\text{cross, DL}}$ and $P_{\text{cross, UL}}$.

Lemma 9: If the transmit power of the RUs/UEs is lower than P_{cross} , MRT or MRC is always better than ZF in terms of sum rate. The power cross point, P_{cross} , at downlink and uplink are given by

$$P_{\text{cross, DL}} = \frac{4}{M - 1},$$

and

$$P_{\text{cross, UL}} = \frac{1}{M - 1}$$

where $K = 2$.

Now we investigate K_{cross} , which is a transceiver mode selection threshold when the transmit power at the transceiver is larger than P_{cross} and when the number of active users varies.

Lemma 10: If the RUs have more transmit power than P_{cross} , the user cross point at downlink, $K_{\text{cross, DL}}$, for selecting a better precoder is given by

$$K_{\text{cross, DL}} = \frac{P_t(M + 1)}{1 + P_t}. \quad (25)$$

If the number of users K is larger than $K_{\text{cross, DL}}$, MRT precoder provides a better sum rate performance.

Proof: Both $\mathcal{R}_{\text{ZFvec, DL}_L}$ and $\mathcal{R}_{\text{MRTmat, DL}_L}$ are concave functions. Also, unlike $\mathcal{R}_{\text{ZFvec, DL}_L}$, $\mathcal{R}_{\text{MRTmat, DL}_L}$ is a monotonic increasing function; thus, two cross points exist: one is when the number of users K is one; the other is when the number of users K has (25) with a large M approximation (this approximation results from satisfying $K_{\text{cross, DL}} = 1$ condition)

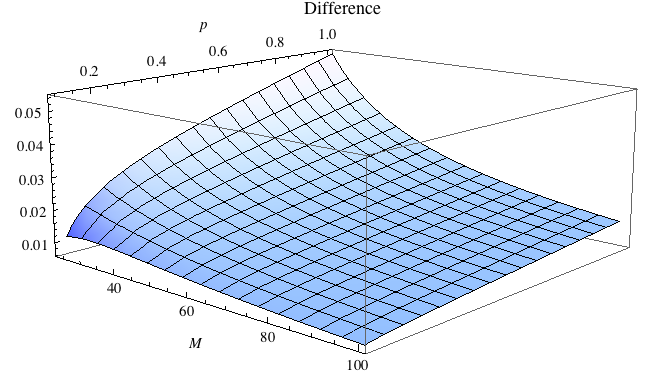


Fig. 3. The difference of the gradient between ZF and MRT at K_{cross} when P is very small (almost zero) and M is much larger than P . The difference is always positive (> 0).

as follows:

$$\begin{aligned} \mathcal{R}_{\text{MRTmat, DL}_L} - \mathcal{R}_{\text{ZFvec, DL}_L} &\geq 0 \\ \Leftrightarrow \frac{P_t(M + 1)}{P_t(K - 1) + K} - \frac{P_t(M - K + 1)}{K} &\geq 0 \\ \approx \frac{P_t M}{P_t(K - 1) + K} - \frac{P_t(M - K + 1)}{K} &\geq 0 \\ \Leftrightarrow K \geq K_{\text{cross, DL}} = \frac{P_t(M + 1)}{1 + P_t}. \end{aligned}$$

Lemma 11: The user cross point, $K_{\text{cross, UL}}$, to select a better receive combining filter at uplink when the RUs have larger transmit power than $P_{\text{cross, UL}}$, is given by

$$K_{\text{cross, UL}} = M + 1 - \frac{1}{P_u}. \quad (26)$$

If the number of users, K , is larger than $K_{\text{cross, UL}}$, MRC provides a better sum rate performance.

Proof: Similar to *Lemma 10*, we can obtain (26) as follows:

$$\begin{aligned} \mathcal{R}_{\text{MRC, UL}_L} - \mathcal{R}_{\text{ZF, UL}_L} &\geq 0 \\ \Leftrightarrow \frac{P_u M}{P_u(K - 1) + 1} - P_u(M - K + 1) &\geq 0 \\ \Leftrightarrow K \geq K_{\text{cross, UL}} = M + 1 - \frac{1}{P_u}. \end{aligned}$$

Lemmas 9-11 provide a proper solution for the low SNR regime like a cell-boundary. For example, if the users have very low SNR, which means P_t or P_u is always lower than $P_{\text{cross, DL}}$ or $P_{\text{cross, UL}}$, the cloud BS should use MRT or MRC to increase a sum rate. Also, the cloud BS should use MRT or MRC for users having transmit power larger than P_{cross} (especially in the low SNR regime) when the number of active users is larger than K_{cross} .

At $K_{\text{cross, DL}}$ in downlink, we check the difference of the gradient between ZF and MRT. If the gradient of ZF is larger than that of MRT, the rate of ZF with vector normalization is larger than that of MRT when $K < K_{\text{cross, DL}}$. In the other case, the rate of MRT with matrix normalization is larger than

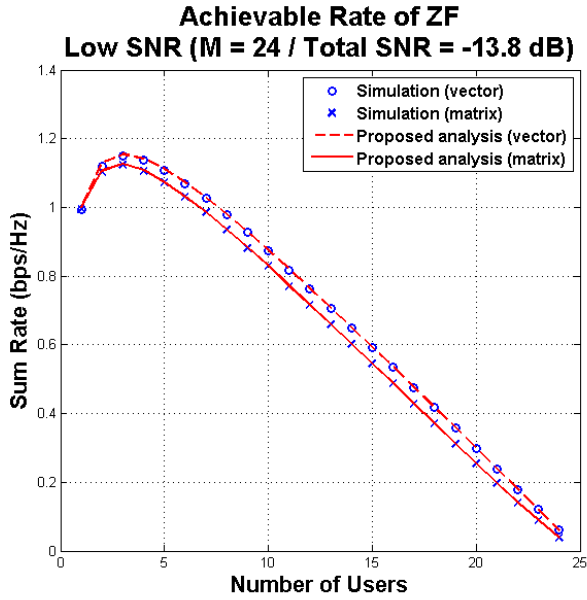


Fig. 4. Achievable rate vs. the number of cell-boundary users, where $M = 24$, $K = [1, 24]$, and total SNR = -13.8 dB.

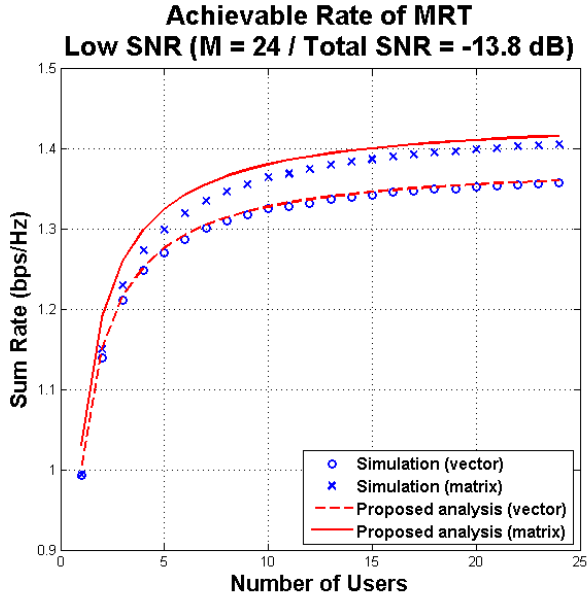


Fig. 5. Achievable rate vs. the number of cell-boundary users, where $M = 24$, $K = [1, 24]$, and total SNR = -13.8 dB.

that of ZF when $K \geq K_{\text{cross, DL}}$. The difference of the gradient between ZF and MRT is expressed as

$$\begin{aligned} & \mathcal{G}_{\text{MRT}_{\text{mat}}, \text{DL}_L} - \mathcal{G}_{\text{ZF}_{\text{vec}}, \text{DL}_L} \\ &= \frac{(P_t + 1)^2}{(M + 1)P \ln 4} - \frac{(M + 1)(P_t + 1)}{MP \ln 2^{(2M+1)}} \end{aligned} \quad (27)$$

where $\mathcal{G}_{\text{MRT}_{\text{mat}}, \text{DL}_L}$ denotes the gradient of the $\mathcal{R}_{\text{MRT}_{\text{mat}}, \text{DL}_L}$ curve at $K_{\text{cross, DL}}$. Similarly, $\mathcal{G}_{\text{ZF}_{\text{vec}}, \text{DL}_L}$ is the gradient of the $\mathcal{R}_{\text{ZF}_{\text{vec}}, \text{DL}_L}^L$ curve at $K_{\text{cross, DL}}$. In general, cell-boundary users have relatively low SNR and, as we assumed, the cloud BS has large-scale antennas, meaning M is much larger than

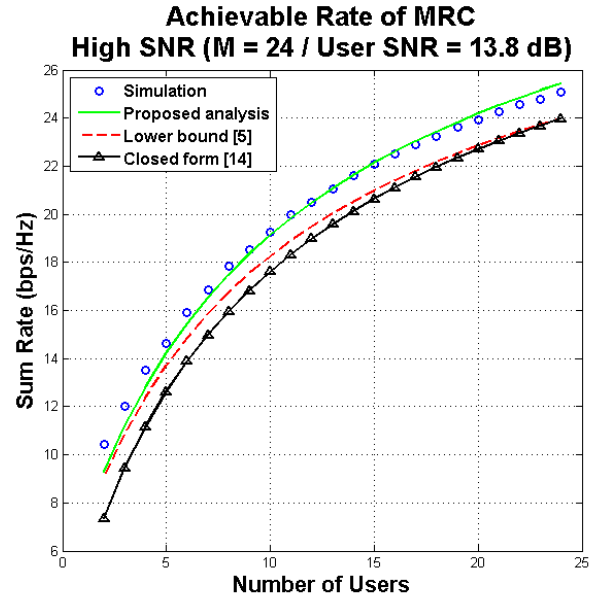


Fig. 6. Achievable rate vs. the number of users at uplink, where $M = 24$, $K = [1, 24]$, and user SNR = 13.8 dB.

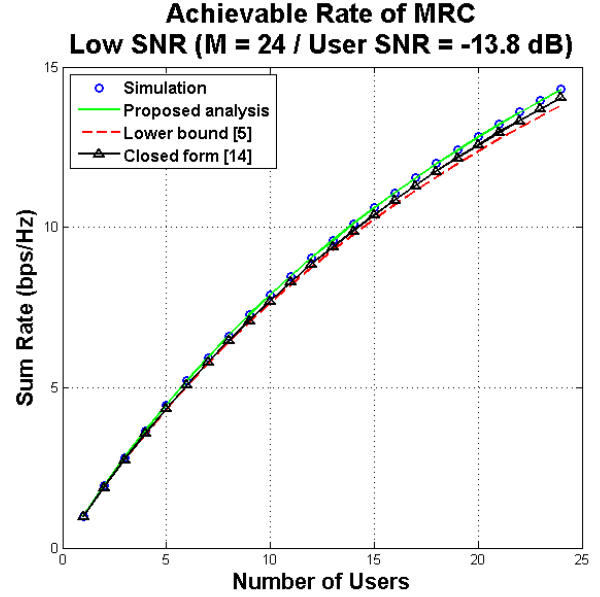


Fig. 7. Achievable rate vs. the number of users at uplink, where $M = 24$, $K = [1, 24]$, and user SNR = -13.8 dB.

P_t . Therefore, if $K_{\text{cross, DL}}$ exists, (27) is always positive. We also confirm this through numerical comparisons as shown in Fig. 3. From this observation, we realize that MRT precoding is suitable for cell-boundary users if the number of active users is larger than $K_{\text{cross, DL}}$.

VII. NUMERICAL RESULTS

For numerical comparisons, we assume that each RU has eight transmit antennas; thus the cloud BS has a total of 24 antennas. *Note that any number of antennas can be used and this constraint is not really related to our system.* This

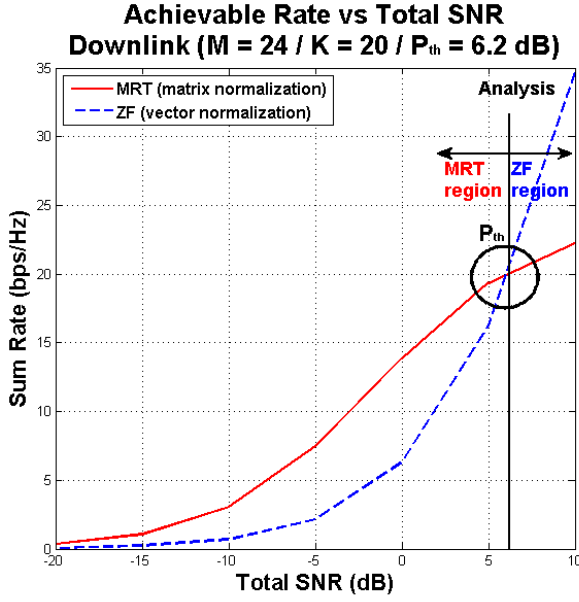


Fig. 8. Achievable sum rate vs total SNR at downlink, where $M = 24$, $K = 20$, and $P_{th} = 6.2$ dB.

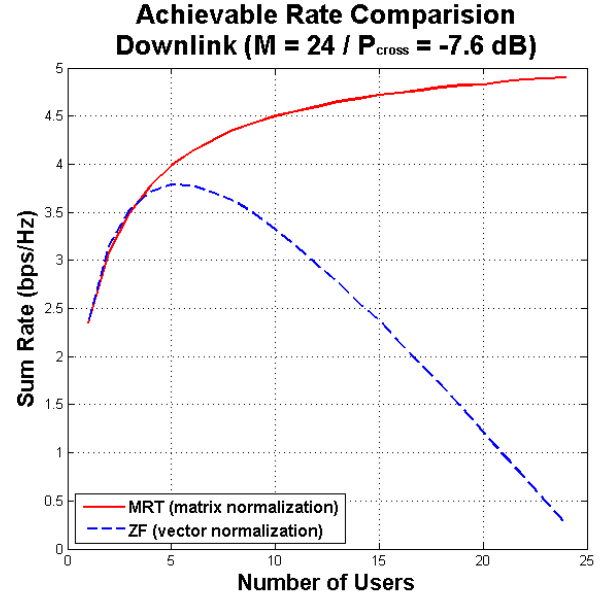


Fig. 10. Achievable rate vs. the number of cell-boundary users at downlink, where $M = 24$, $K = [1, 24]$, $P_t = P_{cross,DL} = -7.6$ dB.

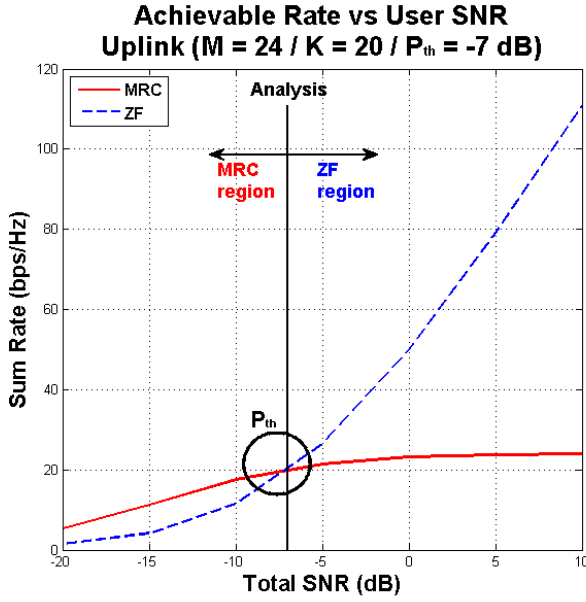


Fig. 9. Achievable sum rate vs user SNR at uplink, where $M = 24$, $K = 20$, and $P_{th} = -7$ dB.

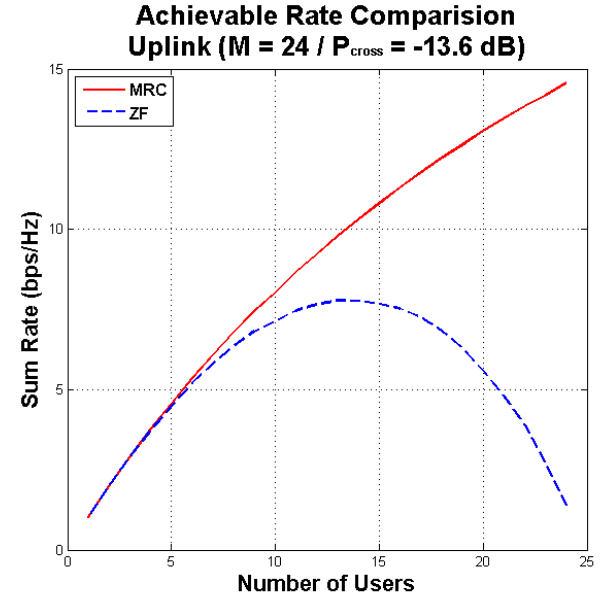


Fig. 11. Achievable rate vs. the number of cell-boundary users at uplink, where $M = 24$, $K = [1, 24]$, $P_u = P_{cross,UL} = -13.6$ dB.

assumption is based on 3GPP LTE-advanced's parameters; Release 10 supports eight Node B antennas [23]. Instead of increasing the number of antennas at each transmitter, we propose using the more feasible cloud concept.

Fig. 4 shows the achievable sum rate of ZF for downlink at low SNR. We compare the simulation results with their theoretical upper bound. As mentioned in Section IV, the ergodic achievable sum rate of ZF with vector normalization approaches its upper bound at low SNR while that of ZF with matrix normalization approaches its first upper bound. Note that *first upper bound* is obtained by Monte

Carlo's simulation because $\mathbb{E} \left\{ \frac{1}{\|F\|_F^2} \right\}$ is unknown. Fig. 5 also describes the achievable sum rate of MRT with $1/M$ (-13.8 dB) total SNR. Our achievable sum rate result is almost the same as the numerical results for vector normalization. There is, however, a gap between the simulation results and the proposed achievable sum rate for matrix normalization. This is because the proposed achievable sum rate form is accurate when there is large M and $P_t \geq 1/M^2$. Our analysis is more accurate than the closed form in [16] which is the same as the lower bound of ZF. From this comparison, we could confirm (as was also shown in Section IV) that ZF

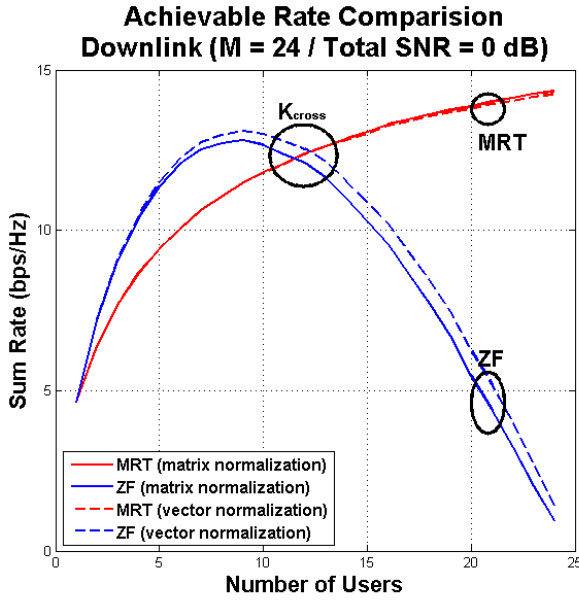


Fig. 12. Achievable rate vs. the number of cell-boundary users, where $M = 24$, $K = [1, 24]$, and total SNR = 0 dB.

with vector normalization is better. In contrast, MRT with matrix normalization is better at getting an improved sum rate performance at low SNR.

Figs. 6 and 7 show that the results from (21) and (22) are approximately the same as the ergodic achievable uplink sum rate of MRC where $P_u \geq M$ and $P_u \leq 1/M$, respectively. Note the large gap between the ergodic achievable uplink sum rate and the lower bound of MRC with finite M shown in [5]. The legend, *Simulation*, indicates the ergodic achievable uplink sum rate of MRC (20) while *Proposed Analysis* in Figs. 6 and 7 indicates the approximation shown in (21) and (22), respectively. Note that the lower bound in [5] is given by

$$\mathcal{R}_{\text{MRC}}^L = K \log_2 \left\{ 1 + \frac{P_u(M-1)}{P_u(K-1)+1} \right\}$$

and the closed form in [16] is given by

$$\mathcal{R}_{\text{MRC}}^L = K \log_2 \left\{ 1 + \frac{P_u M}{P_u K + 1} \right\}.$$

In Fig. 8, we illustrate the achievable sum rate of MRT precoding and ZF precoding at downlink. Fig. 9 illustrates the achievable sum rate of MRC and ZF at uplink ($P_{\text{th}} = 6.2$ dB and -7 dB are calculated by *Lemmas 7* and *8* with $M = 24$ and $K = 20$ at downlink and uplink, respectively). Note that a cross point of MRT (or MRC) curve and ZF curve is the power threshold. It shows that MRC/MRT is better than ZF at low SNR. Figs. 10 and 11 show that MRT/MRC is always better than ZF at very low SNR. Used for simulations were $P_t = P_{\text{cross,DL}} = -7.6$ dB at downlink and $P_u = P_{\text{cross,UL}} = -13.6$ dB at uplink, and $M = 24$. This result verifies *Lemma 9*. We summarize also our conclusions in Tables I, II, and III.

In Fig. 12, we also compare the achievable sum rates of ZF precoding with MRT precoding when the total transmit SNR is 0 dB. It shows that ZF with vector normalization is better

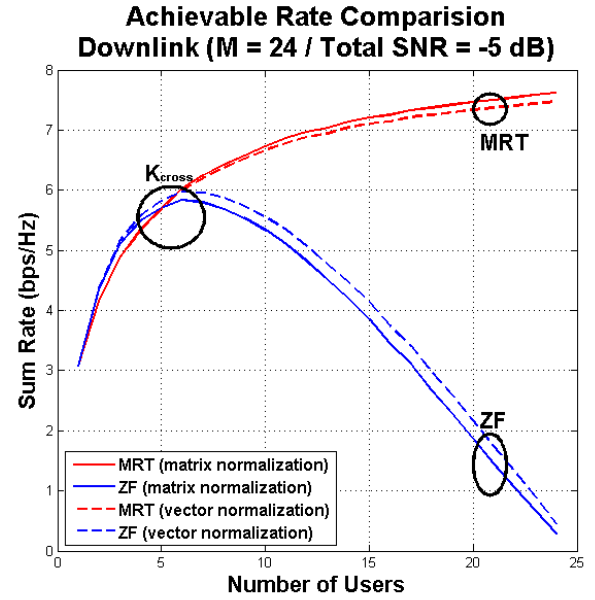


Fig. 13. Achievable rate vs. the number of cell-boundary users, where $M = 24$, $K = [1, 24]$, and total SNR = -5 dB.

while MRT with matrix normalization is better for achieving higher sum rates. Fig. 13 illustrates the achievable sum rates of ZF- and MRT-precoding with -5 dB transmit SNR. The result is similar to that found in Fig. 12. As mentioned in Section VI, in the low SNR regime, using MRT precoding is generally better when the number of active users is larger than $K_{\text{cross, DL}}$. Also, we realize through Figs. 12 and 13 that as SNR decreases, $K_{\text{cross, DL}}$ shifts to the left. This means that the cloud BS could determine a precoding by $K_{\text{cross, DL}}$ at low SNR.

The performance of MRT/MRC increases as K increases while the performance of ZF decreases as K increases. This is because the ergodic sum rate of ZF at $M = K$ goes to a very small constant at downlink, as shown in (12). Similarly, at uplink, the ergodic sum rate of ZF at $M = K$ could also close to a very small value since its lower bound is zero.

VIII. CONCLUSIONS

In this paper, we proposed massive MIMO systems supporting multiple cell-boundary UEs. For precoding designs, we first derived the achievable sum rate bounds of zero-forcing (ZF) and the approximation of the ergodic achievable sum rate of maximum ratio transmission (MRT) with vector/matrix normalization. Through analytical and numerical results, we confirmed that vector normalization is better for ZF while matrix normalization is better for MRT especially at low SNR. We also investigated the optimal mode switching point as functions of the power threshold and the number of active users in a network. According to the mathematical and numerical results the cloud BS can select a transceiver mode to increase the sum rate for both downlink and uplink scenarios. We expect our analysis can give some insights to the industry. In future work, we will consider limited cooperation among RUs and cooperation delay.

TABLE I
PRECODING NORMALIZATION TECHNIQUES IN NETWORK MASSIVE
MIMO SYSTEMS.

| | Precoding normalization technique |
|-----|--|
| ZF | Vector normalization \geq Matrix normalization |
| MRT | Matrix normalization \geq Vector normalization |

TABLE II
OPTIMAL SWITCHING POINT IN NETWORK MASSIVE MIMO SYSTEMS.

| | P_{th} | K_{cross} |
|----------|----------------------------|--------------------------|
| Downlink | $\frac{K^2}{(K-1)(M-K+1)}$ | $\frac{P_t(M+1)}{1+P_t}$ |
| Uplink | $\frac{1}{M-K+1}$ | $M+1-\frac{1}{P_t}$ |

TABLE III
DESIRED TECHNIQUE IN NETWORK MASSIVE MIMO SYSTEMS. ZF
(IF $K \leq K_{cross}$) AND MRT/MRC (IF $K \geq K_{cross}$).

| | K_{cross} | Precoding technique |
|---------------|-------------|---------------------|
| Cell-center | Large | Zero-forcing |
| Cell-boundary | Small | MRT/MRC |

APPENDIX

A. Proof of Lemma 1

Let $h_{k,m}$ be the m -th element of \mathbf{h}_k . Since $h_{k,m}$ is an i.i.d. complex Gaussian random variable with zero mean and unit variance, i.e., $h_{k,m} \sim \mathcal{CN}(0, 1)$, $|h_{k,m}|^2$ is a Gamma random variable with unit shape parameter and unit scale parameter, i.e., $|h_{k,m}|^2 \sim \Gamma(1, 1)$ from the relationship between Rayleigh distribution and Gamma distribution. Therefore, we can say that $|h_{k,m}|^2$ is an exponential random variable with unit parameter ($\lambda = 1$), i.e., $|h_{k,m}|^2 \sim \text{Exp}(1)$ by the property of Gamma distribution and exponential distribution. Since the n -th moment of the exponential random variable is $\frac{n!}{\lambda^n}$, we can obtain $\mathbb{E}(|h_{k,m}|^4) = 2$, $\mathbb{E}(|h_{k,m}|^6) = 6$, and $\mathbb{E}(|h_{k,m}|^8) = 24$.

1) *Proof of Lemma 1. 3*): The expectation of $\|\mathbf{h}_k\|^4$ is given by

$$\begin{aligned}\mathbb{E}(\|\mathbf{h}_k\|^4) &= \mathbb{E}\{|h_{k,1}|^2 + |h_{k,2}|^2 + \dots + |h_{k,M}|^2\}^2 \\ &= M\mathbb{E}(|h_{k,m}|^4) + {}_M P_2 \mathbb{E}(|h_{k,m}|^2 |h_{k,i}|^2) \\ &= M^2 + M\end{aligned}$$

where $i \neq m$. The notation ${}_n P_r$ denotes permutation. The variance of $\|\mathbf{h}_k\|^4$ is also derived by

$$\begin{aligned}\text{Var}(\|\mathbf{h}_k\|^4) &= M\text{Var}(|h_{k,m}|^4) + {}_M P_2 \text{Var}(|h_{k,m}|^2 |h_{k,i}|^2) \\ &\quad + {}_M P_2 \text{Cov}(|h_{k,m}|^2 |h_{k,i}|^2, |h_{k,i}|^2 |h_{k,m}|^2) \\ &\quad + 4{}_M P_2 \text{Cov}(|h_{k,m}|^4, |h_{k,i}|^2 |h_{k,m}|^2) \\ &\quad + 4{}_M P_3 \text{Cov}(|h_{k,m}|^2 |h_{k,i}|^2, |h_{k,m}|^2 |h_{k,j}|^2) \\ &= 4M^3 + 10M^2 + 6M.\end{aligned}\tag{28}$$

The variance terms and the covariance terms in (28) are

calculated by

$$\begin{aligned}\text{Var}(|h_{k,m}|^4) &= 20, \\ \text{Var}(|h_{k,m}|^2 |h_{k,i}|^2) &= 3, \\ \text{Cov}(|h_{k,m}|^2 |h_{k,i}|^2, |h_{k,i}|^2 |h_{k,m}|^2) &= 3, \\ \text{Cov}(|h_{k,m}|^4, |h_{k,i}|^2 |h_{k,m}|^2) &= 4, \\ \text{Cov}(|h_{k,m}|^2 |h_{k,i}|^2, |h_{k,m}|^2 |h_{k,j}|^2) &= 1\end{aligned}$$

where $i \neq j \neq m$.

2) *Proof of Lemma 1. 4*): The expectation of $\|\mathbf{h}_k^* \mathbf{h}_\ell\|^2$ is

$$\begin{aligned}\mathbb{E}(\|\mathbf{h}_k^* \mathbf{h}_\ell\|^2) &= \mathbb{E}(|h_{k,1}^* h_{\ell,1} + h_{k,2}^* h_{\ell,2} + \dots + h_{k,M}^* h_{\ell,M}|^2) \\ &= M\mathbb{E}(|h_{k,m}^* h_{\ell,m}|^2) + {}_M P_2 \mathbb{E}(h_{k,m}^* h_{\ell,m} h_{k,i}^* h_{\ell,i}) \\ &= M\end{aligned}$$

where $i \neq m$. The variance of $\|\mathbf{h}_k^* \mathbf{h}_\ell\|^2$ is also expressed as

$$\begin{aligned}\text{Var}(\|\mathbf{h}_k^* \mathbf{h}_\ell\|^2) &= \text{Var}(|h_{k,1}^* h_{\ell,1} + h_{k,2}^* h_{\ell,2} + \dots + h_{k,M}^* h_{\ell,M}|^2) \\ &= M\text{Var}(|h_{k,m}^* h_{\ell,m}|^2) \\ &\quad + {}_M P_2 \text{Var}(h_{k,m}^* h_{\ell,m} h_{k,i}^* h_{\ell,i}) \\ &= M^2 + 2M\end{aligned}\tag{29}$$

where $\text{Var}(|h_{k,m}^* h_{\ell,m}|^2)$ is 3, and $\text{Var}(h_{k,m}^* h_{\ell,m} h_{k,i}^* h_{\ell,i})$ is 1 ($i \neq m$). Note that the covariance terms in (29) are all zeros.

B. Proof of Ergodic Sum Rate of MRT

First, we suppose the transmit power is smaller than $1/M$ at low SNR ($P_t \leq 1/M$) and it is larger than M at high SNR ($P_t \geq M$) to evaluate the ergodic achievable sum rate of vector normalization. We can then obtain the following equations:

$$P_t \|\mathbf{h}_k\|^2 \approx P_t M\tag{30}$$

at low SNR, and

$$\frac{1}{P_t} \|\mathbf{h}_k\|^2 \approx \frac{1}{P_t} M\tag{31}$$

at high SNR from *Lemmas 1* and *4*.

Next, we assume the transmit power is smaller than $1/M^2$ at low SNR ($P_t \leq 1/M^2$) and larger than M at high SNR ($P_t \geq M$) to evaluate the ergodic achievable sum rate of matrix normalization. Similar to the vector normalization case, we can obtain the following equations:

$$\begin{aligned}P_t \|\mathbf{h}_k\|^4 &\approx P_t (M^2 + M), \\ P_t \|\mathbf{h}_k^* \mathbf{h}_\ell\|^2 &\approx P_t M\end{aligned}\tag{32}$$

at low SNR, and

$$\frac{1}{P_t} \|\mathbf{H}\|_F^2 = \frac{1}{P_t} \sum_{k=1}^K \|\mathbf{h}_k\|^2 \approx \frac{1}{P_t} KM\tag{33}$$

at high SNR.

1) *Proof of (14):*

$$\begin{aligned}
\mathcal{R}_{\text{MRT}_{\text{vec}}, \text{DL-L}} &= \mathbb{E} \left[\sum_{k=1}^K \log_2 \left\{ 1 + \frac{P_t \frac{|\mathbf{h}_k|^4}{\sqrt{K}|\mathbf{h}_k|^2}}{P_t \sum_{\ell=1, \ell \neq k}^K \frac{|\mathbf{h}_k^* \mathbf{h}_\ell|^2}{\sqrt{K}|\mathbf{h}_\ell|^2} + 1} \right\} \right] \\
&= K \mathbb{E} \left[\log_2 \left\{ 1 + \frac{P_t \frac{|\mathbf{h}_k|^2}{K}}{P_t \sum_{\ell=1, \ell \neq k}^K \frac{|\mathbf{h}_k^* \mathbf{h}_\ell|^2}{K|\mathbf{h}_\ell|^2} + 1} \right\} \right] \\
&\stackrel{(a)}{\approx} K \mathbb{E} \left[\log_2 \left\{ 1 + \frac{P_t \frac{M}{K}}{P_t \sum_{\ell=1, \ell \neq k}^K \frac{|\mathbf{h}_k^* \mathbf{h}_\ell|^2}{K|\mathbf{h}_\ell|^2} + 1} \right\} \right] \\
&\stackrel{(b)}{\approx} K \log_2 \left\{ 1 + \frac{P_t \frac{M}{K}}{P_t \sum_{\ell=1, \ell \neq k}^K \frac{\mathbb{E}(|\mathbf{h}_k^* \mathbf{h}_\ell|^2)}{\mathbb{E}(K|\mathbf{h}_\ell|^2)} + 1} \right\} \\
&\stackrel{(c)}{=} K \log_2 \left\{ 1 + \frac{P_t M}{P_t(K-1) + K} \right\}
\end{aligned}$$

where (a) results from (30). Equality (b) and (c) can be obtained by *Lemmas 5* and *1*, respectively.

2) *Proof of (15):*

$$\begin{aligned}
\mathcal{R}_{\text{MRT}_{\text{vec}}, \text{DL-H}} &= \mathbb{E} \left[\sum_{k=1}^K \log_2 \left\{ 1 + \frac{P_t \frac{|\mathbf{h}_k|^4}{\sqrt{K}|\mathbf{h}_k|^2}}{P_t \sum_{\ell=1, \ell \neq k}^K \frac{|\mathbf{h}_k^* \mathbf{h}_\ell|^2}{\sqrt{K}|\mathbf{h}_\ell|^2} + 1} \right\} \right] \\
&= K \mathbb{E} \left[\log_2 \left\{ 1 + \frac{P_t \frac{|\mathbf{h}_k|^4}{K|\mathbf{h}_k|^2}}{P_t \sum_{\ell=1, \ell \neq k}^K \frac{|\mathbf{h}_k^* \mathbf{h}_\ell|^2}{K|\mathbf{h}_\ell|^2} + 1} \right\} \right] \\
&\stackrel{(d)}{\approx} K \mathbb{E} \left[\log_2 \left\{ 1 + \frac{P_t \frac{|\mathbf{h}_k|^4}{KM}}{P_t \sum_{\ell=1, \ell \neq k}^K \frac{|\mathbf{h}_k^* \mathbf{h}_\ell|^2}{KM} + 1} \right\} \right] \\
&\stackrel{(e)}{\approx} K \log_2 \left\{ 1 + \frac{P_t(M+1)}{P_t(K-1) + K} \right\}
\end{aligned}$$

where (d) results from (31) and (e) can be obtained by *Lemmas 1* and *5*.

3) *Proof of (16): in the low SNR regime*

$$\begin{aligned}
\mathcal{R}_{\text{MRT}_{\text{mat}}, \text{DL-L}} &= \mathbb{E} \left[\sum_{k=1}^K \log_2 \left\{ 1 + \frac{P_t \frac{|\mathbf{h}_k|^4}{\|\mathbf{H}\|_F^2}}{P_t \sum_{\ell=1, \ell \neq k}^K \frac{|\mathbf{h}_k^* \mathbf{h}_\ell|^2}{\|\mathbf{H}\|_F^2} + 1} \right\} \right] \\
&= K \mathbb{E} \left[\log_2 \left\{ 1 + \frac{P_t |\mathbf{h}_k|^4}{P_t \sum_{\ell=1, \ell \neq k}^K |\mathbf{h}_k^* \mathbf{h}_\ell|^2 + \|\mathbf{H}\|_F^2} \right\} \right] \\
&\stackrel{(f)}{\approx} K \mathbb{E} \left[\log_2 \left\{ 1 + \frac{P_t(M^2 + M)}{P_t \sum_{\ell=1, \ell \neq k}^K M + \|\mathbf{H}\|_F^2} \right\} \right] \\
&\stackrel{(g)}{\approx} K \log_2 \left\{ 1 + \frac{P_t(M+1)}{P_t(K-1) + K} \right\}
\end{aligned}$$

where (f) can be obtained by using (32) directly. Equality (g) can also be derived by *Lemma 5* and $\mathbb{E}(\|\mathbf{H}\|_F^2) = MK$.

4) *Proof of (16): in the high SNR regime:*

$$\begin{aligned}
\mathcal{R}_{\text{MRT}_{\text{mat}}, \text{DL-H}} &= \mathbb{E} \left[\sum_{k=1}^K \log_2 \left\{ 1 + \frac{P_t \frac{|\mathbf{h}_k|^4}{\|\mathbf{H}\|_F^2}}{P_t \sum_{\ell=1, \ell \neq k}^K \frac{|\mathbf{h}_k^* \mathbf{h}_\ell|^2}{\|\mathbf{H}\|_F^2} + 1} \right\} \right] \\
&= K \mathbb{E} \left[\log_2 \left\{ 1 + \frac{|\mathbf{h}_k|^4}{\sum_{\ell=1, \ell \neq k}^K |\mathbf{h}_k^* \mathbf{h}_\ell|^2 + \frac{1}{P_t} \|\mathbf{H}\|_F^2} \right\} \right] \\
&\stackrel{(h)}{\approx} K \mathbb{E} \left[\log_2 \left\{ 1 + \frac{|\mathbf{h}_k|^4}{\sum_{\ell=1, \ell \neq k}^K |\mathbf{h}_k^* \mathbf{h}_\ell|^2 + \frac{1}{P_t} MK} \right\} \right] \\
&\stackrel{(i)}{\approx} K \log_2 \left\{ 1 + \frac{P_t(M+1)}{P_t(K-1) + K} \right\}
\end{aligned}$$

where (h) results from (33) while (i) can be obtained by *Lemmas 1* and *5* as well.

C. Proof of Ergodic Sum Rate of MRC

1) *Proof of (21):*

$$\begin{aligned}
\mathcal{R}_{\text{MRC}, \text{UL-H}} &= \mathbb{E} \left[K \log_2 \left\{ 1 + \frac{P_u |\mathbf{h}_k|^4}{P_u \sum_{\ell=1, \ell \neq k}^K |\mathbf{h}_k^* \mathbf{h}_\ell|^2 + |\mathbf{h}_k|^2} \right\} \right] \\
&= \mathbb{E} \left[K \log_2 \left\{ 1 + \frac{|\mathbf{h}_k|^4}{\sum_{\ell=1, \ell \neq k}^K |\mathbf{h}_k^* \mathbf{h}_\ell|^2 + \frac{1}{P_u} |\mathbf{h}_k|^2} \right\} \right] \\
&\approx \mathbb{E} \left[K \log_2 \left\{ 1 + \frac{|\mathbf{h}_k|^4}{\sum_{\ell=1, \ell \neq k}^K |\mathbf{h}_k^* \mathbf{h}_\ell|^2 + \frac{1}{P_u} M} \right\} \right] \\
&\approx K \log_2 \left\{ 1 + \frac{P_u(M+1)}{P_u(K-1) + 1} \right\}. \tag{34}
\end{aligned}$$

using (30), (31), *Lemmas 1* and *5* where $P_u \geq M$.

2) *Proof of (22):*

$$\begin{aligned}
\mathcal{R}_{\text{MRC}, \text{UL-L}} &= \mathbb{E} \left[K \log_2 \left\{ 1 + \frac{P_u |\mathbf{h}_k|^4}{P_u \sum_{\ell=1, \ell \neq k}^K |\mathbf{h}_k^* \mathbf{h}_\ell|^2 + |\mathbf{h}_k|^2} \right\} \right] \\
&= \mathbb{E} \left[K \log_2 \left\{ 1 + \frac{P_u |\mathbf{h}_k|^2}{P_u \sum_{\ell=1, \ell \neq k}^K \frac{|\mathbf{h}_k^* \mathbf{h}_\ell|^2}{|\mathbf{h}_k|^2} + 1} \right\} \right] \\
&\approx \mathbb{E} \left[K \log_2 \left\{ 1 + \frac{P_u M}{P_u \sum_{\ell=1, \ell \neq k}^K \frac{|\mathbf{h}_k^* \mathbf{h}_\ell|^2}{|\mathbf{h}_k|^2} + 1} \right\} \right] \\
&\approx K \log_2 \left\{ 1 + \frac{P_u M}{P_u(K-1) + 1} \right\}
\end{aligned}$$

using the same methods as in (34) where $P_u \leq \frac{1}{M}$.

REFERENCES

- [1] D. Gesbert, M. Kountouris, R. W. Heath, Jr., C.-B. Chae, and T. Salzer, "Shifting the MIMO paradigm: From single user to multiuser communications," *IEEE Sig. Proc. Mag.*, vol. 24, no. 5, pp. 36–46, Oct. 2007.
- [2] Q. Spencer, A. L. Swindlehurst, and M. Haardt, "Zero-forcing methods for downlink spatial multiplexing in multiuser MIMO channels," *IEEE Trans. Sig. Proc.*, vol. 52, pp. 462–471, Feb. 2004.
- [3] C.-B. Chae, D. Mazzarese, N. Jindal, and R. W. Heath, Jr., "Coordinated beamforming with limited feedback in the MIMO broadcast channel," *IEEE Jour. Select. Areas in Comm.*, vol. 26, no. 8, pp. 1505–1515, Oct. 2008.

- [4] C.-B. Chae and R. W. Heath, Jr., "On the optimality of linear multiuser MIMO beamforming for a two-user two-input multiple-output broadcast system," *IEEE Sig. Proc. Lett.*, vol. 16, no. 2, pp. 117–120, Feb. 2009.
- [5] H. Q. Ngo, E. G. Larsson, and T. L. Marzetta, "Energy and spectral efficiency of very large multiuser MIMO systems," *IEEE Trans. Comm.*, vol. 61, no. 4, pp. 1436–1449, April 2012.
- [6] T. L. Marzetta, "Noncooperative cellular wireless with unlimited numbers of base station antennas," *IEEE Trans. Wireless Comm.*, vol. 9, no. 11, pp. 3590–3600, Nov. 2010.
- [7] F. Rusek, D. Persson, B. K. Lau, E. G. Larsson, T. L. Marzetta, O. Edfors, and F. Tufvesson, "Scaling up MIMO: Opportunities and challenges with large arrays," *IEEE Sig. Proc. Mag.*, vol. 30, no. 1, pp. 40–60, Jan. 2013.
- [8] C.-B. Chae, S. Kim, and R. W. Heath, Jr., "Network coordinated beamforming for cell-boundary users: Linear and non-linear approaches," *IEEE Jour. Select. Topics in Sig. Proc.*, vol. 3, no. 6, pp. 1094–1105, Dec. 2009.
- [9] C.-B. Chae, I. Hwang, R. W. Heath, Jr., and V. Tarokh, "Interference aware-coordinated beamforming in a multi-cell system," *IEEE Trans. Wireless Comm.*, vol. 11, no. 10, pp. 3692–3703, Oct. 2012.
- [10] H. Huh, G. Caire, H. C. Papadopoulos, and S. A. Ramprasad, "Achieving massive MIMO spectral efficiency with a not-so-large number of antennas," *IEEE Trans. Wireless Comm.*, vol. 11, no. 9, pp. 3226–3239, Sep. 2012.
- [11] J. Jose, A. Ashikhmin, T. L. Marzetta, and S. Vishwanath, "Pilot contamination and precoding in multi-cell TDD systems," *IEEE Trans. Wireless Comm.*, vol. 10, no. 8, pp. 2640–2651, Aug. 2011.
- [12] J. Nam, J.-Y. Ahn, A. Adhikary, and G. Caire, "Joint spatial division and multiplexing: Realizing massive MIMO gains with limited channel state information," in *Proc. of Conf. on Info. Scien. and Systems*, March 2012, pp. 1–6.
- [13] M. Filippou, D. Gesbert, and H. Yin, "Decontaminating pilots in cognitive massive MIMO networks," in *Proc. of Int. Symp. on Wireless Comm. Systems*, Aug. 2012, pp. 816–820.
- [14] H. Yang and T. L. Marzetta, "Performance of conjugate and zero-forcing beamforming in large-scale antenna systems," *IEEE Jour. Select. Areas in Comm.*, vol. 31, no. 2, pp. 172–179, 2013.
- [15] H. Huh, A. M. Tulino, and G. Caire, "Network MIMO with linear zero-forcing beamforming: Large system analysis, impact of channel estimation, and reduced-complexity scheduling," *IEEE Trans. Info. Th.*, vol. 58, no. 5, pp. 2911–2934, May 2012.
- [16] J. Hoydis, S. ten Brink, and M. Debbah, "Massive MIMO in the UL/DL of cellular networks: How many antennas do we need?" *IEEE Jour. Select. Areas in Comm.*, vol. 31, no. 2, pp. 160–171, Feb. 2013.
- [17] A. M. Tulino and S. Verdú, "Random matrix theory and wireless communications," *Foundations and Trends in Comm. and Info. Th.*, vol. 1, no. 1, 2004.
- [18] G. Caire, N. Jindal, M. Kobayashi, and N. Ravindran, "Multiuser MIMO achievable rates with downlink training and channel state feedback," *IEEE Trans. Info. Th.*, vol. 56, no. 6, pp. 2845–2866, June 2010.
- [19] R. H. Y. Louie, M. R. McKay, and I. B. Collings, "Maximum sum-rate of MIMO multiuser scheduling with linear receivers," *IEEE Trans. Comm.*, vol. 57, no. 11, pp. 3500–3510, Nov. 2009.
- [20] I. S. Gradshteyn and I. M. Ryzhik, *Table of Integrals, Series, and Products*. Academic Press, 2007.
- [21] K. K. Wong and Z. Pan, "Array gain and diversity order of multiuser MISO antenna systems," *Int. J. Wireless Inf. Networks*, vol. 2008, no. 15, pp. 82–89, May 2008.
- [22] C. B. Peel, B. M. Hochwald, and A. L. Swindlehurst, "A vector-perturbation technique for near-capacity multiantenna multiuser communication-part I: channel inversion and regularization," *IEEE Trans. Comm.*, vol. 53, no. 1, pp. 195–202, Jan. 2005.
- [23] S. Sesia, I. Toufik, and M. Baker, *LTE, The UMTS Long Term Evolution: From Theory to Practice*. Wiley, 2012.

PLACE
PHOTO
HERE

Yeon-Geun Lim (S'12) received his B.S. degree in Information and Communications Engineering from Sungkyunkwan University, Korea in 2011. He is now with the School of Integrated Technology, Yonsei University, Korea and is working toward the Ph.D. degree.

His research interest includes massive MIMO and interference management techniques for smart small cell networks.

PLACE
PHOTO
HERE

Chan-Byoung Chae (S'06 - M'09 - SM'12) is an Assistant Professor in the School of Integrated Technology, College of Engineering, Yonsei University, Korea. He was a Member of Technical Staff (Research Scientist) at Bell Laboratories, Alcatel-Lucent, Murray Hill, NJ, USA from 2009 to 2011. Before joining Bell Laboratories, he was with the School of Engineering and Applied Sciences at Harvard University, Cambridge, MA, USA as a Post-Doctoral Research Fellow. He received the Ph. D. degree in Electrical and Computer Engineering from

The University of Texas (UT), Austin, TX, USA in 2008, where he was a member of the Wireless Networking and Communications Group (WNCG).

Prior to joining UT, he was a Research Engineer at the Telecommunications R&D Center, Samsung Electronics, Suwon, Korea, from 2001 to 2005. While having worked at Samsung, he participated in the IEEE 802.16e standardization, where he made several contributions and filed a number of related patents from 2004 to 2005. His current research interests include capacity analysis and interference management in energy-efficient wireless mobile networks and nano (molecular) communications. He serves as an Editor for the IEEE TRANS. ON WIRELESS COMMUNICATIONS and IEEE/KICS JOUR. COMM. NETS. He is an IEEE Senior Member.

Dr. Chae was the recipient/co-recipient of the IEEE Signal Processing Best Paper Award in 2013, the IEEE ComSoc AP Outstanding Young Researcher Award in 2012, the IEEE VTS Dan. E. Noble Fellowship Award in 2008, the Gold Prize (1st) in the 14th/19th Humantech Paper Contests, and the KSEA-KUSCO scholarship in 2007. He also received the Korea Government Fellowship (KOSEF) during his Ph. D. studies.

PLACE
PHOTO
HERE

Giuseppe Caire (S'92 - M'94 - SM'03 - F'05) was born in Torino, Italy, in 1965. He received the B.Sc. in Electrical Engineering from Politecnico di Torino (Italy), in 1990, the M.Sc. in Electrical Engineering from Princeton University in 1992 and the Ph.D. from Politecnico di Torino in 1994. He was a recipient of the AEI G.Someda Scholarship in 1991, has been with the European Space Agency (ESTEC, Noordwijk, The Netherlands) from May 1994 to February 1995, was a recipient of the COTRAO Scholarship in 1996 and of a CNR Scholarship in

1997. He has been visiting Princeton University in Summer 1997 and Sydney University in Summer 2000. He has been Assistant Professor in Telecommunications at the Politecnico di Torino, Associate Professor at the University of Parma, Italy, Professor with the Department of Mobile Communications at the Eurecom Institute, Sophia-Antipolis, France, and he is currently a professor of Electrical Engineering with the Viterbi School of Engineering, University of Southern California, Los Angeles, CA. He served as Associate Editor for the IEEE TRANSACTIONS ON COMMUNICATIONS in 1998-2001 and as Associate Editor for the IEEE TRANSACTIONS ON INFORMATION THEORY in 2001-2003. He received the Jack Neubauer Best System Paper Award from the IEEE Vehicular Technology Society in 2003, and the IEEE Communications Society & Information Theory Society Joint Paper Award in 2004 and in 2011. Giuseppe Caire is Fellow of IEEE since 2005. He has served in the Board of Governors of the IEEE Information Theory Society from 2004 to 2007, and as President of the IEEE Information Theory Society in 2011. His main research interests are in the field of communications theory, information theory, channel and source coding with particular focus on wireless communications.